Electrochemical Behavior of Novel Ti/IrO_x−Sb_2O_5−SnO_2 Anodes

Guohua Chen,* Xueming Chen, and Po Lock Yue

Department of Chemical Engineering, The Hong Kong University of Science and Technology, Clear Water Bay, Kowloon, Hong Kong, China

Received: September 17, 2001; In Final Form: February 15, 2002

There are growing interests in anodes for oxygen evolution because of the importance of this reaction in many electrochemical processes such as water electrolysis, electroplating, electrosynthesis, metal electrowinning, and electroflotation. Ternary IrO_x−Sb_2O_5−SnO_2 has been shown to be among the best elecytrocatalysts for oxygen evolution. Its high stability and relatively low cost will make it more attractive than IrO_x and many other electrocatalytic materials. In this paper, the open-circuit potential, voltammetric behavior, oxygen evolution mechanism, and kinetics of the IrO_x−Sb_2O_5−SnO_2 coated titanium anodes were studied. It was found that the open-circuit potential could change significantly during the initial period of time probably because of the hydration of the coating film. Cyclic voltammograms obtained on Ti/IrO_x−Sb_2O_5−SnO_2 were somewhat different from those on IrO_x coated anodes. Apparent cathodic peaks from Ir(III)/Ir(IV) and Ir(IV)/Ir(V) were observed. However, the corresponding anodic peaks were very weak. Voltammetric investigation also showed that Ti/IrO_x−Sb_2O_5−SnO_2 could provide fast electron transfer. Despite high anodic stability, severe damage occurred when a Ti/IrO_x−Sb_2O_5−SnO_2 electrode was cathodically polarized. An O_2 evolution mechanism involving cyclic formation and decomposition of $\equiv IrO_2$ was proposed. The Tafel slope and $\partial E/\partial \log a_{H^+}$ obtained were 86 and 45 mV dec^{-1}, respectively.

Introduction

Since the discovery of dimensionally stable anodes (DSA) by Beer,[1,2] considerable efforts have been devoted toward the development of various novel oxide coatings to reach better anode compositions for catalyzing different electrochemical reactions. Industrial anodes have been customarily based on RuO_2−TiO_2 mixtures, where RuO_2 is an active component and TiO_2 is a stabilizing agent.[3] However, because of easy conversion of RuO_2 to unstable RuO_4 at high anodic potential, the service life of RuO_2−TiO_2 is unacceptably low for oxygen evolution.[4]

Over the past decade, substituting RuO_2 with IrO_x in DSA has received much attention. A major technological advantage of the IrO_x-based coatings over the more common ruthenium−titanium mixed oxide coating is their ability to evolve oxygen in strongly acidic environments while maintaining good catalytic activity and dimensional stability.[5] In general, Ta_2O_5, TiO_2, SnO_2, and ZrO_2 are used as stabilizing or dispersing agents in IrO_x-based DSAs.[5−9] Occasionally, a third component such as CeO_2 is also added.[10,11] It should be noted that although incorporation of Ta_2O_5 and TiO_2, etc. can save IrO_x loading and improve the coating stability, the requirement of molar percentage of the precious Ir component is still very high. The optimal IrO_x contents are 80 mol % for IrO_x−ZrO_2, 70 mol % for IrO_x−Ta_2O_5, and 40 mol % for IrO_x−TiO_2, below which electrode service lives decrease sharply.[7]

There are many factors that can affect electrode stability. One important factor is the coating conductivity. Low conductivity will result in a high electric field inside the coating and thus cause a quick migration of O^{2-} ions toward the substrate. The quick O^{2-} migration may then accelerate formation of an insulating TiO_2 layer at the interface between the titanium substrate and the coating, leading to electrode passivation. Lower electrode stability at lower mol % IrO_x for most IrO_x-based coatings is, more often than not, associated with insufficient coating conductivity. Comninellis and Vercesi[7] have analyzed the microstructures of IrO_x−TiO_2, IrO_x−ZrO_2, and IrO_x−Ta_2O_5 by XRD. It was found that the miscibility of IrO_x with TiO_2, ZrO_2, and Ta_2O_5 was rather poor. Actually, an oxide coating was simply a mixture of the IrO_x crystals and the dispersing agent particles that might dissolve a limited amount of IrO_x. Because TiO_2, ZrO_2, and Ta_2O_5 are poor in conductivity, it can be concluded that electric conduction inside the oxide coatings is achieved by chains of the conductive IrO_x crystals as proposed by Roginskaya et al.[12] for RuO_2−TiO_2. This is essentially the mechanism of conduction of cermets.[13] Obviously, in all coatings mentioned above, if IrO_x contents are not sufficient, the chains become interrupted, and the conductivity drops significantly. This is the reason most IrO_x-based oxide mixtures need high mol % IrO_x.

In our previous work,[14] a novel ternary IrO_x−SnO_2−Sb_2O_5 electrocatalyst containing only 10 mol % IrO_x had been investigated for oxygen evolution. In this oxide mixture, SnO_2 serves as a dispersing agent, Sb_2O_5 serves as a dopant, and IrO_x serves as a catalyst. Its good conductivity, compact structure, and high homogeneity with metastable solid solution nature make it more stable than IrO_x. The service lives of the IrO_x−SnO_2−Sb_2O_5-coated titanium electrodes are predicted to be over nine years in application under 0.1 A cm^{-2} in strong acidic solutions.

The objectives of the present study are to investigate the basic electrochemical properties of theTi/IrO_x−Sb_2O_5−SnO_2 anodes and to explore the mechanism and kinetics of oxygen evolution on them.

* To whom correspondence should be addressed. Phone: (852)23587138. Fax: (852)23580054. E-mail: kechengh@ust.hk.

10.1021/jp013547o CCC: $22.00
Published on Web 04/04/2002

Experimental Section

Chemicals. All chemicals, including $SnCl_4 \cdot 5H_2O$ (98+%, Acros, NJ), $SbCl_3$ (99+%, Acros, NJ), iridium (IV) chloride hydrate (53.89% Ir, Strem Chemicals, MA), K_2SO_4 (Nacalai Tesque, Kyoto, Japan), potassium ferrocyanide (99%, Sigma, MO), potassium ferricyanide (99%, Sigma, MO), 2-propanol (99.7%, Lab-scan, Bangkok, Thailand), hydrochloric acid (37%, Riedel-deHaen, Seelze, German), and sulfuric acid (98%, Acros, NJ) were used as received. Electrolyte solutions were prepared using 0.05 μs cm^{-1} deionized water.

Electrodes Preparation. Titanium cylinders, 5.3 mm long and 12 mm in diameter with an effective area of 2 cm^2, were used as substrates. The electrodes were prepared by a thermal decomposition method. Prior to coating, the titanium substrates underwent sandblasting, tap water washing, 10 minutes of ultrasonic cleaning in deionized water, 2 min of etching in boiling 37% hydrochloric acid, and another 10 minutes of ultrasonic cleaning in deionized water. After pretreatment, the titanium substrates were first brushed at room temperature with the precursor which had a molar ratio of Ir:Sb:Sn = 10:10:80 using the mixture of 2-propanol and concentrated hydrochloric acid as solvents, dried at 80 °C for 5 min to allow solvents to vaporize, and then baked at 550 °C for 5 min. This procedure was repeated 15−18 times. Finally the electrodes were annealed at 550 °C for an hour. The total oxide loading of the prepared electrodes was 15 gm^{-2}. More details of the preparation procedure can be found elsewhere.[14]

Electrochemical Measurement. All electrochemical experiments were performed with a standard three-electrode cell (RDE0018, EG&G) and a potentiostat/galvanostat (PGSTAT 100, Autolab, Netherlands). Pt wire was used as a counter-electrode, and Ag/AgCl/saturated KCl (0.222 V vs SHE) with a Luggin capillary was used as a reference-electrode. Electrode potentials are quoted with respect to SHE. The resistances between a working electrode and the Luggin capillary were measured using the frequency response analyzer of the potentiostat/galvanostat. The ohmic drops in the solutions were compensated. Solutions were purged before electrochemical experiments with nitrogen gas. The open-circuit potential was examined in aqueous H_2SO_4 solutions. Cyclic voltammetry was carried out in both 0.5 M H_2SO_4 and solution of 10−200 mM $[Fe(CN)_6]^{3-}$/$[Fe(CN)_6]^{4-}$ (1:1) and 0.2 M K_2SO_4. In the kinetics investigation, the potential−current data were potentiostatically obtained under quasistationary states at a scan rate of 0.002 V s^{-1}. To reduce the variation of activity coefficients caused by the change of acid concentrations, saturated K_2SO_4 was added to maintain a relatively steady ionic strength of the electrolyte solutions.

Results and Discussion

Open-Circuit Potential. The open-circuit potential (E_{oc}) can provide some information on the state of the electrode surface.[10] When a Ti/ IrO_x−Sb_2O_5−SnO_2 electrode was inserted into a 0.5 M H_2SO_4 solution, the initial E_{oc} was measured to be 0.72 V as shown in Figure 1. Within 10 minutes, however, E_{oc} decreased rapidly to 0.63 V. Subsequently, E_{oc} varied slowly and the steady E_{oc} reached was about 0.60 V. Actually, E_{oc} is the mixed potential of varieties of redox couples possibly present in the electrode and the solution, including not only the coating species such as Ir(IV)/Ir(IV), Sb(V)/Sb(III), and Sn(IV)/Sn(II) but also TiO_2/Ti from the substrate. At an open-circuit state, although no net current passes through the external circuit, redox reactions are still taking place at the electrode. Usually, E_{oc} is not determined by the thermodynamic equilibrium potentials but by the kinetics of the individual reactions. The variation of E_{oc} reflects the change of the electrode surface properties probably resulting from hydration.

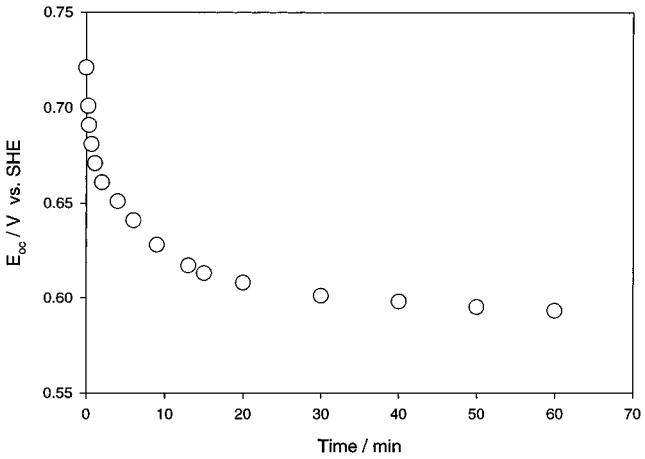

Figure 1. Variation of open-circuit potential with time after a new Ti/IrO_x−$Sb_2O_5SnO_2$ electrode was inserted in a 0.5 M H_2SO_4 solution.

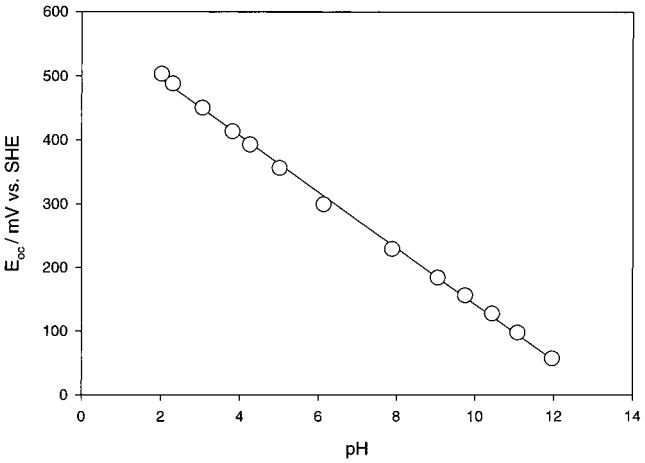

Figure 2. Dependence of the steady open-circuit potential on pH.

It has been reported that IrO_x films can be used as pH sensing material because of their good chemical stability over a wide range of pH and temperature in aqueous solutions.[15,16] In an attempt to examine if IrO_x−Sb_2O_5−SnO_2 is also able to serve this purpose, the dependence of E_{oc} obtained after reaching a steady state on pH was investigated, and the results are shown in Figure 2. Good linearity was obtained, indicating high quality of IrO_x−Sb_2O_5−SnO_2 for use as pH sensing material. However, the slope obtained was −45 mV pH^{-1}, lower in magnitude than literature values ranging from −59 to −80 mV pH^{-1} for IrO_x films.[15−18]

Voltammetric Behavior in 0.5 M H_2SO_4 Solution. Figure 3 shows cyclic voltammograms obtained on Ti/IrO_x−Sb_2O_5−SnO_2 in 0.5 M H_2SO_4 solution. In the first a few scan cycles, the voltammogram changes dramatically as observed on Ti/SnO_2−Sb_2O_5 [19] and Ti/IrO_x [20] probably as a consequence of further hydration of the coating surface.[21] The shape of voltammograms obtained on Ti/IrO_x−Sb_2O_5−SnO_2 then becomes consistent quickly. After 100 cycles, the voltammograms keep almost identical, compared to Ti/SnO_2−Sb_2O_5 and Ti/IrO_x which cannot reach consistent cyclic voltammograms until several hundreds of cycles.[19,20] This is attributed to the extremely high electrochemical stability of Ti/IrO_x−Sb_2O_5−SnO_2.[14]

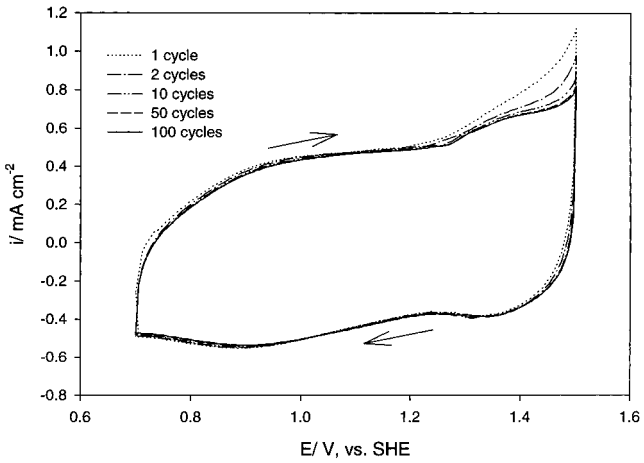

Figure 3. Development of cyclic voltammograms with cycles in 0.5 M H_2SO_4 at a scan rate of 100 mV s^{-1}.

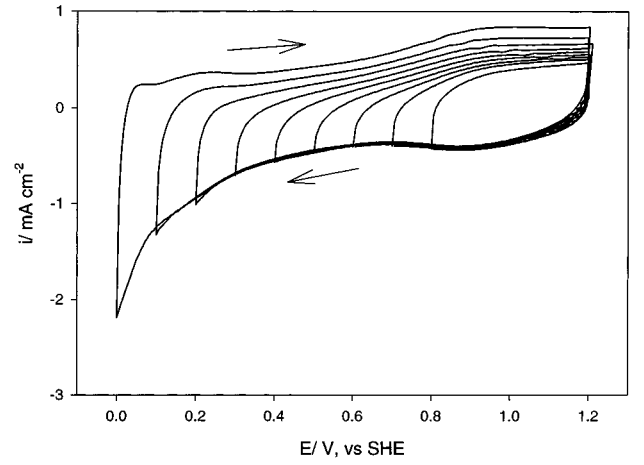

Figure 4. Change of cyclic voltammograms with lower potential limit in 0.5 M H_2SO_4 solution at a scan rate of 100 mV s^{-1}.

During the potential scan, the oxidation states of iridium may change, and thus, well-defined current peaks can usually be identified on IrO_x coated electrodes. Huppauff and Lengeler[16] clearly observed the anodic and cathodic peaks from the redox-couples of Ir(III)/Ir(IV) and Ir(IV)/Ir(V) on IrO_x films deposited on glass substrates. A similar result was reported by Petit and Plichon[22] who used conducting transparent SnO_2-coated glass as substrates. However, Mousty et al.[20] could only detect the anodic and cathodic peaks from Ir(III)/Ir(IV) and the cathodic peak from Ir(IV)/Ir(V) on the Ti/IrO_x electrode prepared by induction heating, whereas the anodic peak from Ir(IV)/Ir(V) was hardly noticeable. For the $Ti/IrO_x-Sb_2O_5-SnO_2$ electrode, very broad cathodic current peaks around 0.90 and 1.35 V were observed from Figure 3. They were attributed to the reductions from Ir(IV) to Ir(III) and Ir(V) to Ir(IV).[20,22] However, the corresponding anodic current peaks were very weak. Actually, anodic current increased monotonically with the potential until about 1.35 V where a small kink was observed. This is probably associated with overlapping the anodic current peak of Ir(III)/Ir(IV) by that of Ir(IV)/Ir(V).

Figure 4 shows voltammograms obtained by fixing the upper potential limit at 1.2 V and decreasing the lower potential limit in steps of 0.10 V. As the potential scan limit is extended to the lower potential region, the redox reactions of Sb(III)/Sb(V) and Sn(II)/Sn(IV) occurred. It was noticed that the cathodic current varied almost along the same curve, whereas the anodic

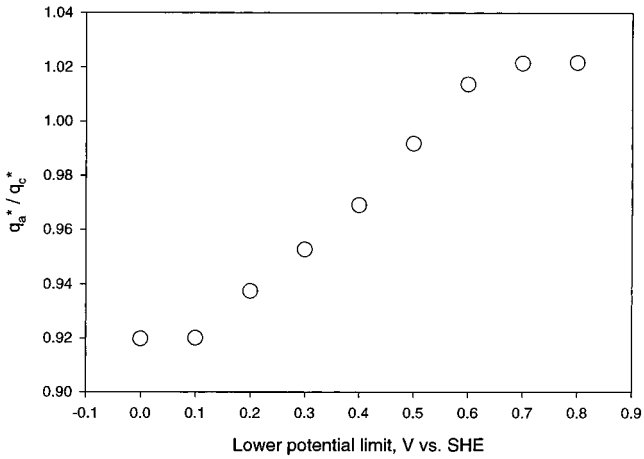

Figure 5. Dependence of the anodic-to-cathodic voltammetric charge ratio on lower potential limit at fixed upper potential limit of 1.20 V vs SHE.

currents increased as the lower potential limit dropped. A possible explanation is the significant irreversibility of the Sb(III)/Sb(V) and Sn(II)/Sn(IV) redox couples. Because of the difficulty in oxidizing Sb(III) and Sn(II) in the lower potential region in the positive scan direction, conversion of Sb(III) and Sn(II) to Sb(V) and Sn(IV) continued in the higher potential region, which contributed part of anodic current, leading to an increase in the total anodic current.

Figure 5 demonstrates the anodic-to-cathodic voltammetric charge ratio, q^*_a/q^*_c, at a different potential scan range corresponding to Figure 4. As the lower limit of the scan potential dropped, the q^*_a/q^*_c deviated from 1 and decreased linearly until the lower potential limit of 0.1 V. Such a variation of q^*_a/q^*_c further demonstrates the irreversibility of the conversion of the Sb and Sn species. To examine whether the conversion of the Sb and Sn species from higher to lower oxidation states will affect the electrochemical stability of the $IrO_x-Sb_2O_5-SnO_2$ catalyst, a $Ti/IrO_x-Sb_2O_5-SnO_2$ electrode was subjected to a cathodic polarization galvanostatically at 0.02 A cm^{-2}. After half an hour, it was found that severe damage of the coating film occurred and loose oxide powder could be removed easily from the titanium substrate surface. This suggests that $Ti/IrO_x-Sb_2O_5-SnO_2$ electrodes can only be used as anodes and care must be taken in applications to avoid any electrode polarity mistake of wrong connection.

Voltammetric investigation was also conducted on a well-polarized electrode. A voltammogram comparison is shown in Figure 6 between the as-prepared electrode and the one polarized in 3 M H_2SO_4 solution under a current density as high as 1 A cm^{-2} at 35 °C for 1000 h. Both electrodes showed a similar voltammogram shape. However, the polarized one had a much higher capacitance charging current than the as-prepared one. It is generally believed that the charge storage of iridium oxide films results from both a double-layer capacitance and a pseudocapacitance arising from the faradaic process of Ir species.[20] The situation of the $IrO_x-Sb_2O_5-SnO_2$ film should be similar. The double-layer capacitance is dependent on the real surface area of the film. Because $IrO_x-Sb_2O_5-SnO_2$ has a compact structure, with rare cracks and pores,[14] a significant increase in the real surface area of the coating film after polarization is impossible, and the increased charging current observed on the polarized electrode must be from the increase in the pseudocapacitance. Because electron transfer can take place in the whole thickness of the oxide layer where the Ir sites are accessible,[20] the pseudocapacitance increase is believed

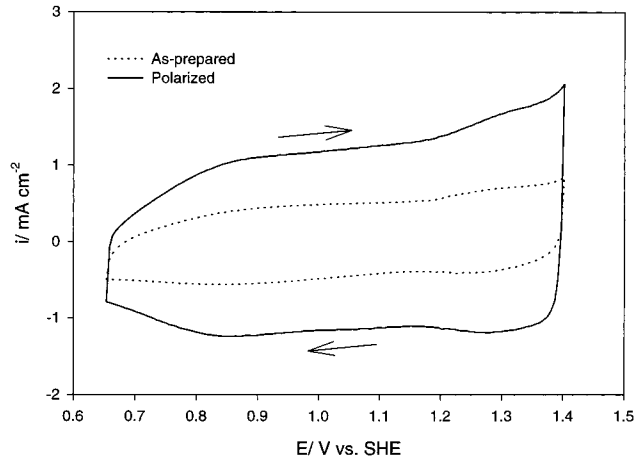

Figure 6. Voltammogram comparison between as-prepared and polarized electrodes in 0.5 M H_2SO_4 solution at a scan rate of 100 mV s^{-1}.

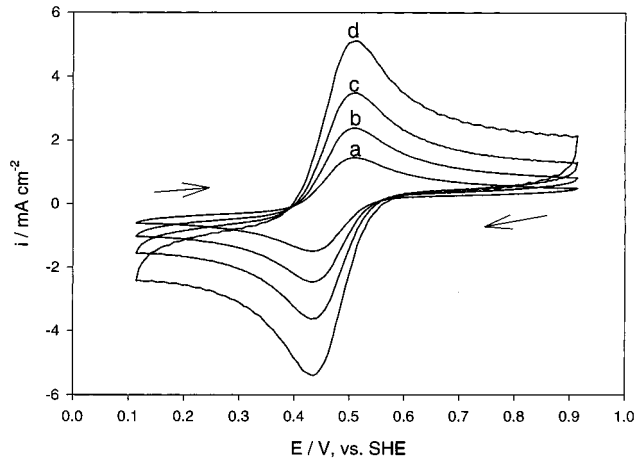

Figure 7. Cyclic voltammograms obtained in 10 mM $[Fe(CN)_6]^{3-}$ + 10 mM $[Fe(CN)_6]^{4-}$ + 0.2 M K_2SO_4 solution at different scan rates. (a) 20, (b) 50, (c) 100, and (d) 200 mV s^{-1}.

to be caused by the extension of Ir sites involved in the faradaic process from the outer to the inner oxide layer. Such an extension or coating structure modification is the direct result of the long time of polarization. Obviously, the increased pseudocapacitance cannot bring about any enhancement in oxygen evolution. This is simply because oxygen evolution takes place at the interface between the coating surface and the electrolyte solution, not involving any internal Ir sites. In reality, as the polarization proceeded at a constant current, the anodic potential did not drop but rose slightly during the initial period of polarization. This can be explained by the increase in the real current density because of the decrease in the electrode surface area after partial dissolution of the sharp edges of the original oxide crystals.

Voltammetric Behavior for the $[Fe(CN)_6]^{3-}/[Fe(CN)_6]^{4-}$ Redox Couple. To examine the electron-transfer rate on $Ti/IrO_x-Sb_2O_5-SnO_2$, the voltammetric behavior of the $[Fe(CN)_6]^{3-}/[Fe(CN)_6]^{4-}$ redox couple was studied. Cyclic voltammograms obtained in the solution with a concentration of 10 mM for both $Fe(CN)_6]^{3-}$ and $[Fe(CN)_6]^{4-}$ at steady state under different scan rates are shown in Figure 7. Each voltammogram shows a well-defined anodic peak at 0.50 V and a corresponding cathodic peak at 0.44 V. $i_{panodic}$ is equal to $i_{pcathodic}$. The peak separation value is about 60 mV and not significantly subjected to the scan rate. Moreover, there is a good linearity between the peak current density and the square root of the scan rate as shown in Figure 8, indicating that the redox reaction is under diffusion control. All of these features demonstrate that the redox reaction of the $[Fe(CN)_6]^{3-}/[Fe(CN)_6]^{4-}$ couple at the $Ti/IrO_x-Sb_2O_5-SnO_2$ electrode is reversible.

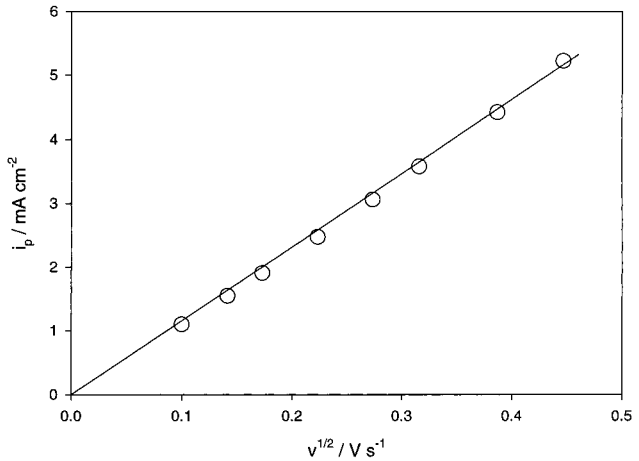

Figure 8. Dependence of anodic peak current density on scan rate in a 10 mM $[Fe(CN)_6]^{3-}$ + 10 mM $[Fe(CN)_6]^{4-}$ + 0.2 M K_2SO_4 solution.

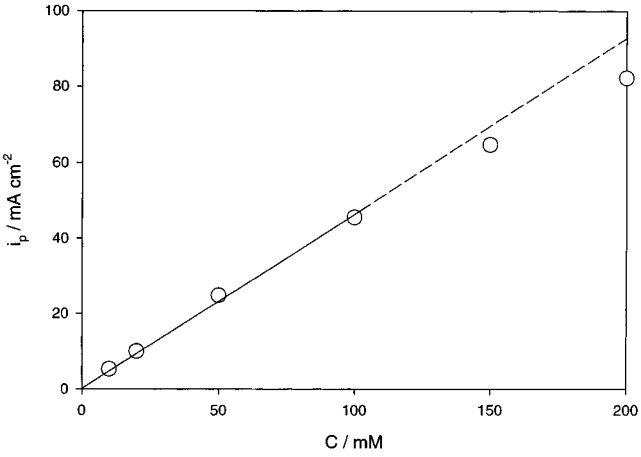

Figure 9. Dependence of anodic peak current density on concentration of $[Fe(CN)_6]^{3-}/[Fe(CN)_6]^{4-}$ (1:1) at a scan rate of 200 mV s^{-1}. Supporting electrolyte: 0.2 M K_2SO_4.

The voltammetry of the $[Fe(CN)_6]^{3-}/[Fe(CN)_6]^{4-}$ redox couple on $Ti/IrO_x-Sb_2O_5-SnO_2$ was also investigated under higher concentrations. The anodic peak current density was proportional to concentration, which revealed that the redox reaction was under diffusion control, up to $[Fe(CN)_6]^{3-}$ = $[Fe(CN)_6]^{4-}$ = 100 mM as shown in Figure 9. Even when the concentration was as high as 200 mM, the anodic peak current density deviated only slightly from a linear relationship, indicating $Ti/IrO_x-Sb_2O_5-SnO_2$ electrodes could provide fast electron transfer.

Mechanism and Kinetics of O_2 Evolution in Acidic Solutions. A number of researchers have studied the mechanism of oxygen evolution on IrO_x films. It has been established that IrO_x can hydrate easily in aqueous solution to form iridium hydrous oxide. However, a clearly defined oxide−solution interface may not exist, and the iridium hydrous oxide layer may substantially consist of polymeric oxide chains that contain a fairly high concentration of coordinated OH and H_2O species.[23,24] Iwakura et al.[25] believed that O_2 evolution at IrO_x films in acid solution involves formation of absorbed OH species, followed by a series of unclear processes. However, Kotz et al.[26] presented a different pathway which involves cyclic

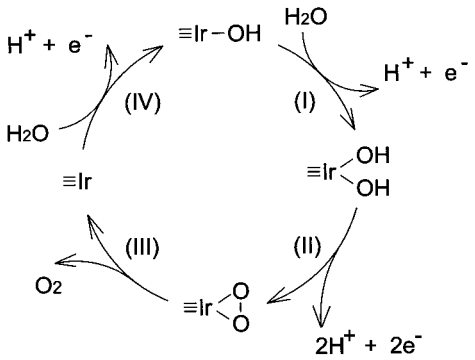

Figure 10. Proposed model of oxygen evolution on Ti/ $IrO_x-Sb_2O_5-SnO_2$ electrodes.

formation and decomposition of IrO_3:

$$Ir(OH)_3 \rightleftarrows IrO(OH)_2 + H^+ + e^- \quad (1)$$

$$IrO(OH)_2 \rightleftarrows IrO_2(OH) + H^+ + e^- \quad (2)$$

$$IrO_2(OH) \rightleftarrows IrO_3 + H^+ + e^- \quad (3)$$

$$IrO_3 + H_2O \rightleftarrows \frac{1}{2}O_2 + IrO(OH)_2 \quad (4)$$

The ternary $IrO_x-Sb_2O_5-SnO_2$ can be regarded as a combination of IrO_x and $Sb_2O_5-SnO_2$. Because $Sb_2O_5-SnO_2$ has a very high overpotential for oxygen evolution,[27,28] the oxygen evolution on Ti/ $IrO_x-Sb_2O_5-SnO_2$ should be predominantly carried out on the active Ir sites. However, what needs to be emphasized here is (1) $IrO_x-Sb_2O_5-SnO_2$ exists in the form of a metastable solid solution and (2) the IrO_x content in the $IrO_x-Sb_2O_5-SnO_2$ coating is only 8.2 mol %.[14] These two facts indicate that the Ir species in the $IrO_x-Sb_2O_5-SnO_2$ coating may be highly dispersed. In other words, the active Ir sites are separated from each other in space. Therefore, it is speculated that the two O atoms in the O_2 molecule are most likely split simultaneously from the same active site. On the basis of the analysis above, a mechanism for oxygen evolution on the Ti/ $IrO_x-Sb_2O_5-SnO_2$ anodes is presented and shown schematically in Figure 10.

Step II involves a two-electron transition. It should be much more difficult than those involving only a one-electron transition and thus supposed to be the rate-determining step. The kinetic equations can be written as follows:

$$i = Fk_1q_1 \exp\left[\frac{\beta_1 FE}{RT}\right] - Fk_{-1}q_2a_{H^+} \exp\left[\frac{-(1-\beta_1)FE}{RT}\right] = Fk_2q_2 \exp\left[\frac{\beta_2 FE}{RT}\right] \quad (5)$$

where k_1 and k_{-1} are the forward and backward reaction rate constants for step I, k_2 is the forward reaction rate constant for step II, q_1 and q_2 are the molar fraction of $\equiv Ir(OH)_2$ and $\equiv IrO_2$ on the coating surface, β_1 and β_2 are symmetric factors, and E is the potential.

At relatively high current density, assume that $\equiv Ir(OH)_2$ is dominant, namely, $q_1 \approx 1$, and reaction I is at quasiequilibrium state, then q_2 is obtained as:

$$q_2 = \frac{k_1}{k_{-1}} \frac{\exp\left[\frac{FE}{RT}\right]}{a_{H^+}} \quad (6)$$

Substitute the value of q_2 into eq 5

$$i = F\frac{k_1k_2}{k_{-1}a_{H^+}} \exp\left[\frac{(1+\beta_2)FE}{RT}\right] \quad (7)$$

As oxygen evolves, part of the active sites may lose their activity because of adsorption of O_2 molecules, leading to a decrease in current density. To compensate such an effect, an impacting factor ϕ is introduced. Therefore, eq 7 is rewritten as

$$i = \phi F\frac{k_1k_2}{k_{-1}a_{H^+}} \exp\left[\frac{(1+\beta_2)FE}{RT}\right] \quad (8)$$

It is believed that OH groups on a metal oxide surface can behave as weak Brønsted acids to dissociate in aqueous solution to release protons.[29] Hence, the coating property and the reaction constants may change slightly as a_{H^+} changes. Assuming power law relations of ϕ with i, and k_1k_2/k_{-1} with a_{H^+}, that is

$$\phi = \frac{K_1}{i^m} \quad (9)$$

$$\frac{k_1k_2}{k_{-1}} = \frac{K_2}{a_{H^+}{}^n} \quad (10)$$

where K_1, K_2, m, and n are constants. Then the electrode potential E can be expressed as

$$E = K + 2.303\frac{RT(1+m)}{(1+\beta_2)F}\log i + 2.303\frac{RT(1+n)}{(1+\beta_2)F}\log a_{H^+} \quad (11)$$

where $K = 2.303[RT \log(K_1K_2F)]/[(1+\beta_2)F]$

Equation 11 demonstrates the linear dependence of E on log i and log a_{H^+}, with slopes

$$\frac{\partial E}{\log i} = 2.303\frac{RT(1+m)}{(1+\beta_2)F} \quad (12)$$

and

$$\frac{\partial E}{\partial \log a_{H^+}} = 2.303\frac{RT(1+n)}{(1+\beta_2)F} \quad (13)$$

Figure 11 displays the E vs log i plot in 0.5 M H_2SO_4 solution. As expected, large deviation from linearity is observed at lower current density. Essentially, when the current density is small, the backward rate of the reaction I is much slower than that of the corresponding forward rate because of the lower concentration of $\equiv IrO_2$. In such a case, the reaction I is not at a quasiequilibrium state and accordingly the theoretical model (11) is no longer valid. Beyond 1 mA cm^{-2}, however, good linear relationship between E and log i is obtained, in agreement with the theoretical model. The Tafel slope obtained is 86 mV dec^{-1}, compared to 56−160 mV dec^{-1} for the IrO_x coated electrodes.[5,25,30]

Figure 12 shows the E vs log a_{H^+} plots at different current densities. Good linearity between E and log a_{H^+} is also observed for all cases in the wide a_{H^+} range from 0.01 to 1.0 M, again in agreement with the theoretical model (11). The slope, namely, $\partial E/\partial \log a_{H^+}$, was found to be around 45 mV dec^{-1}, consistent with that obtained at the open-circuit state.

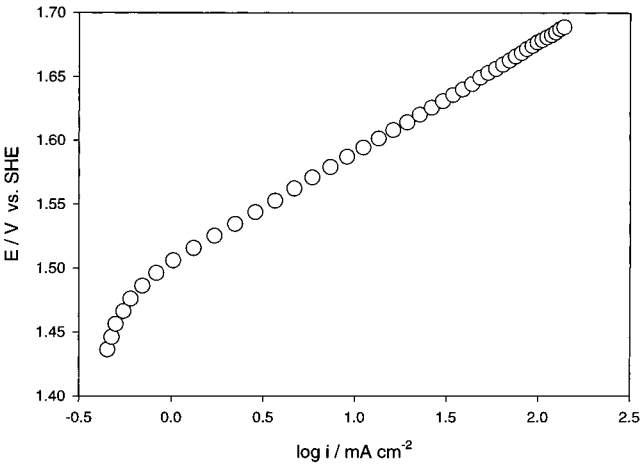

Figure 11. Dependence of potential on current density in 0.5 M H_2SO_4 solution at 25 °C.

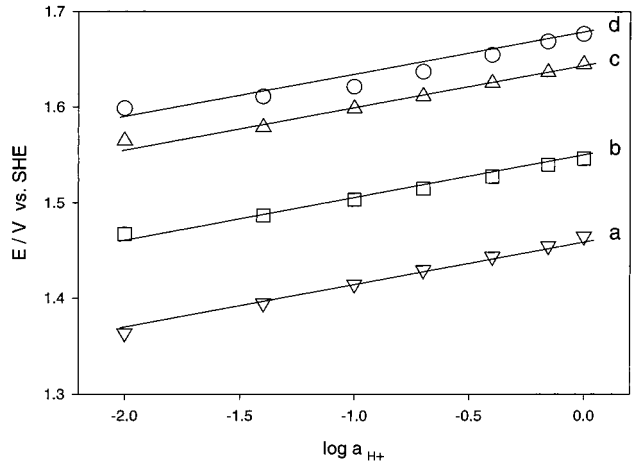

Figure 12. Dependence of potential on a_{H^+} at 25 °C under different current density. (a) 0.1, (b) 1.0, (c) 10, and (d) 20 mA cm^{-2}.

Assuming $\beta_2 = 0.5$, m and n are calculated to be 1.19 and 0.15, respectively, on the basis of the kinetic experimental data.

Conclusions

In this study, the basic electrochemical properties of Ti/ IrO_x−Sb_2O_5−SnO_2 were measured. It was found that the open-circuit potential could change significantly during initial period of time probably because of the hydration of the coating film. Reproducible voltammograms could be obtained quickly, further revealing high electrochemical stability of the Ti/IrO_x−Sb_2O_5−SnO_2 electrodes. Like IrO_x coated electrodes, Ti/IrO_x−Sb_2O_5−SnO_2 showed noticed pseudocapacitance charge storage nature. Broad cathodic current peaks around 0.90 V for Ir(IV)/Ir(III) and 1.35 V for Ir(V)/Ir(IV) were detected. However, the corresponding anodic current peaks were too weak to notice. It was found that the charge storage could be enhanced after polarization in 3 M H_2SO_4 solution at 1 A cm^{-2} for 1000 h presumably by extending Ir sites involved in the faradaic process from the outer to inner oxide layer because of coating structure modification. Despite high stability as anodes, Ti/IrO_x−Sb_2O_5−SnO_2 electrodes could be damaged quickly when used as cathodes. The voltammetric investigation of the $[Fe(CN)_6]^{3-}$/$[Fe(CN)_6]^{4-}$ redox couple on Ti/IrO_x−Sb_2O_5−SnO_2 electrodes demonstrated reversible characteristics. An O_2 evolution mechanism involving cyclic formation and decomposition of $\equiv IrO_2$ was proposed. The Tafel slope and $\partial E/\partial \log a_{H^+}$ obtained were 86 and 45 mV dec^{-1}, respectively.

Acknowledgment. The authors are grateful to the financial support by Hong Kong Research Grant Council under the Project HKUST6248/02P.

References and Notes

(1) Beer, H. B. U.S. Patent 3,632,498, 1972.
(2) Beer, H. B. *J. Electrochem. Soc.* **1980**, *127*, 303C.
(3) Trasatti, S.; Lodi, G. In *Electrodes of conductive metallic oxides, Part B*; Trasatti, S., Ed.; Elsevier: Amsterdam, The Netherlands, 1981; p 521.
(4) Hine, F.; Yasuda, M.; Noda, T.; Yoshida, T.; Okuda, J. *J. Electrochem. Soc.* **1979**, *126*, 1439.
(5) Balko, E. N.; Nguyen, P. H. *J. Appl. Electrochem.* **1991**, *21*, 678.
(6) Rolewicz, J.; Comninellis, Ch.; Plattner, E.; Hinden, J. *Electrochim. Acta* **1988**, *33*, 573.
(7) Comninellis, Ch.; Vercesi, G. P. *J. Appl. Electrochem.* **1991**, *21*, 335.
(8) Vercesi, G. P.; Rolewicz, J.; Comninellis, Ch. *Thermochim. Acta* **1991**, *176*, 31.
(9) Cardarelli, F.; Taxil, P.; Savall, A.; Comninellis, Ch.; Manoli, G.; Leclerc, O. *J. Appl. Electrochem.* **1998**, *28*, 245.
(10) Alves, V. A.; Silva, L. A. D.; Boodts, J. F. C.; Trasatti, S. *Electrochim. Acta* **1994**, *39*, 1585.
(11) Alves, V. A.; Silva, L. A. D.; Oliveira; E. D.; Boodts, J. F. C. *Mater. Sci. Forum* **1998**, *289*−*292*, 655.
(12) Roginskaya, Yu. E.; Galyamov, B. Sh.; Belova, I. D.; Shifrina, R. R.; Kozhevnikov, V. B.; Bystrov, V. I. *Elektrokhimiya* **1982**, *18*, 1327.
(13) Abeles, B.; Pinch, H. L.; Gittleman, J. I. *Phys. Rev. Lett.* **1975**, *35*, 247.
(14) Chen, X. M.; Chen, G. H.; Yue, P. L. *J. Phys. Chem. B* **2001**, *5*, 4623.
(15) Burke, L. D.; Mulcahy, J. K.; Whelan, D. P. *J. Electroanal. Chem.* **1984**, *163*, 117.
(16) Huppauff, M.; Lengeler, B. *J. Electrochem. Soc.* **1993**, *140*, 598.
(17) Hitchman, M. L.; Ramanathan, S. *Analyst* **1988**, *113*, 35.
(18) Olthuis, W.; Robben, M. A. M.; Bervoeld, P.; Bos, M.; van der Linden, W. E. *Sens. Actuators* **1990**, *B2*, 247.
(19) Correa-Lozano, B.; Comninellis, Ch.; Battisti, A. D. *J. Appl. Electrochem.* **1996**, *26*, 683.
(20) Mousty, C.; Foti, G.; Comninellis, Ch.; Reid, V. *Electrochim. Acta* **1999**, *45*, 451.
(21) Ardizzone, S.; Fregonara, G.; Trasatti, S. *J. Electroanal. Chem.* **1989**, *266*, 191.
(22) Petit, M. A.; Plichon, V. *J. Electroanal. Chem.* **1998**, *444*, 247.
(23) Burke, L. D.; Whelan, D. P. *J. Electroanal. Chem.* **1984**, *162*, 121.
(24) O'Sullivan, E. J. M.; Calvo, E. J. In *Comprehensive Chemical Kinetics*; Compton, R. G., Ed.; Elsevier: Amsterdam, The Netherlands, 1987; p 247.
(25) Iwakura, C.; Tada, H.; Tamura, H. *Denki Kagfaku* **1977**, *45*, 202.
(26) Kotz, R.; Neff, H.; Stucki, S. *J. Electrochem. Soc.* **1984**, *131*, 72.
(27) Kotz, R.; Stucki, S.; Carcer, B. *J. Appl. Electrochem.* **1991**, *21*, 14.
(28) Lipp, L.; Pletcher, D. *Electrochim. Acta* **1997**, *42*, 1091.
(29) Trasatti, S. *Electrochim. Acta* **1984**, *29*, 1503.
(30) Matsumoto, Y.; Tazawa, T.; Muroi, N.; Sato, E. *J. Electrochem. Soc.* **1986**, *133*, 2257.